RSC Mechanochemistry

ROYAL SOCIETY OF CHEMISTRY

PAPER

View Article Online
View Journal | View Issue

Cite this: *RSC Mechanochem.*, 2024, **1**, 367

Total mechano-synthesis of 2-cyclopropyl-4-(4-fluorophenyl)quinoline-3-acrylaldehyde—a pivotal intermediate of pitavastatin†

Jingbo Yu, *[ab] Yanhua Zhang,[a] Zehao Zheng[a] and Weike Su *[ab]

Received 18th April 2024
Accepted 27th June 2024

DOI: 10.1039/d4mr00036f

rsc.li/RSCMechanochem

Pitavastatin (PTV), a potent cholesterol-lowering agent, holds considerable commercial appeal, driving chemists to fervently pursue its efficient and sustainable synthesis. Despite prolonged efforts over several decades, the quest for a simplified, more efficacious, and environmentally conscious manufacturing process for PTV remains a significant challenge. Our study introduces a three-step total mechano-synthesis, commencing with readily available 4-bromoquinoline, to produce the key intermediate (2-cyclopropyl-4-(4-fluorophenyl)quinoline-3-acrylaldehyde) of PTV. This methodology incorporates an extrusive Suzuki–Miyaura coupling, mechanochemical Minisci C–H alkylation, and extrusive oxidation Heck coupling, each thoroughly presented to display their scalability. Notably, we emphasize the extensive exploration of substrate versatility in Minisci reactions to access cyclopropane-bearing pharmaceutical compounds and natural products. This total mechano-synthesis route distinguishes itself through eco-friendly reaction conditions, exceptional stepwise efficiency, intuitive operability, and pronounced potential for large-scale implementation, paving the way for PTV's streamlined and sustainable manufacture.

Introduction

Pitavastatin (PTV), approved by the FDA in 2009, is commonly referred to as a "Superstatin" in the pharmaceutical industry due to its excellent therapeutic effects and small dosage.[1] Acting as an HMG-CoA reductase inhibitor, its prominent efficacy is depicted by the increase of high-density lipoprotein cholesterol and the reduction of low-density lipoprotein cholesterol.[2] Besides its lipid-lowering effects, PTV exhibits pleiotropic effects like anti-inflammatory, immunomodulatory, and antithrombotic activities.[3] Over recent decades, the preparation of PTV drug has garnered persistent attention.[4] Apart from heptanoate as the basic structure, a core quinoline ring assembled with fluorophenyl and cyclopropyl moieties provides improved pharmacokinetics and effective HMG-CoA inhibition at low doses. Central to accessing PTV is the synthesis of 2-cyclopropyl-4-(4-fluorophenyl)quinoline-3-acrylaldehyde, which serves as the key intermediate **7a** (Scheme 1a). Typically, this intermediate is initially derived from polysubstituted quinoline formaldehyde II *via* a Wittig reaction,[5] a well-established synthetic pathway for introducing the C=C bonds group, albeit challenged by the generation of significant amounts of phosphine oxide byproduct, leading to low atom economy efficiency. Besides, the synthetic methods for quinoline formaldehyde II always necessitate multiple functional group preinstallations[6a–f] and the use of toxic and hazardous chemicals such as PBr_3,[6d] acyl chloride[6e] and concentrated sulfuric acid,[6f] which result in low overall efficiency and cause numerous environmental concerns. Therefore, the development of a novel and green synthetic route with competitive advantages is highly appealing.

In recent years, research on essentially solvent-free methodologies for organic synthesis using mechanochemistry[7] has gained popularity due to its potential to eliminate or significantly reduce the need for solvent, enhance reaction rates, and offers alternative selectivity. The application of mechanochemical techniques in the synthesis for drug molecule has proven to be a more environmentally friendly and sustainable approach compared to conventional synthesis pathways. Recent advancements in medicinal mechanochemistry have witnessed many successful cases,[8] wherein active pharmaceutical ingredients (APIs) are synthesized entirely *via* mechanochemical methods. These include Phenytoin[8d] (antiepileptic drug), CEDMH[8e]/CADMH[8f] (antiseptic), Glibenclamide[8g]/Chlorpropamide[8g] (hypoglycemic drugs), Procainamide[8h] (anti-arrhythmia agent), Paracetamol[8h] (antipyretic analgesic), Axitinib[8i]

[a]*Laboratory of Pharmaceutical Engineering of Zhejiang Province, Key Laboratory for Green Pharmaceutical Technologies and Related Equipment of Ministry of Education, Collaborative Innovation Center of Yangtze River Delta Region Green Pharmaceuticals, Zhejiang University of Technology, Hangzhou, 310014, P. R. China. E-mail: yjb@zjut.edu.cn*

[b]*Huzhou Key Laboratory of Mechanochemistry, Zhejiang Yangtze River Delta Biomedical Industry Technology Research Park, Deqing, 313200, P. R. China*

† Electronic supplementary information (ESI) available: Experimental procedures, optimization data, environmental factor (*E*-factor) calculation, characterization data and NMR spectra. See DOI: https://doi.org/10.1039/d4mr00036f

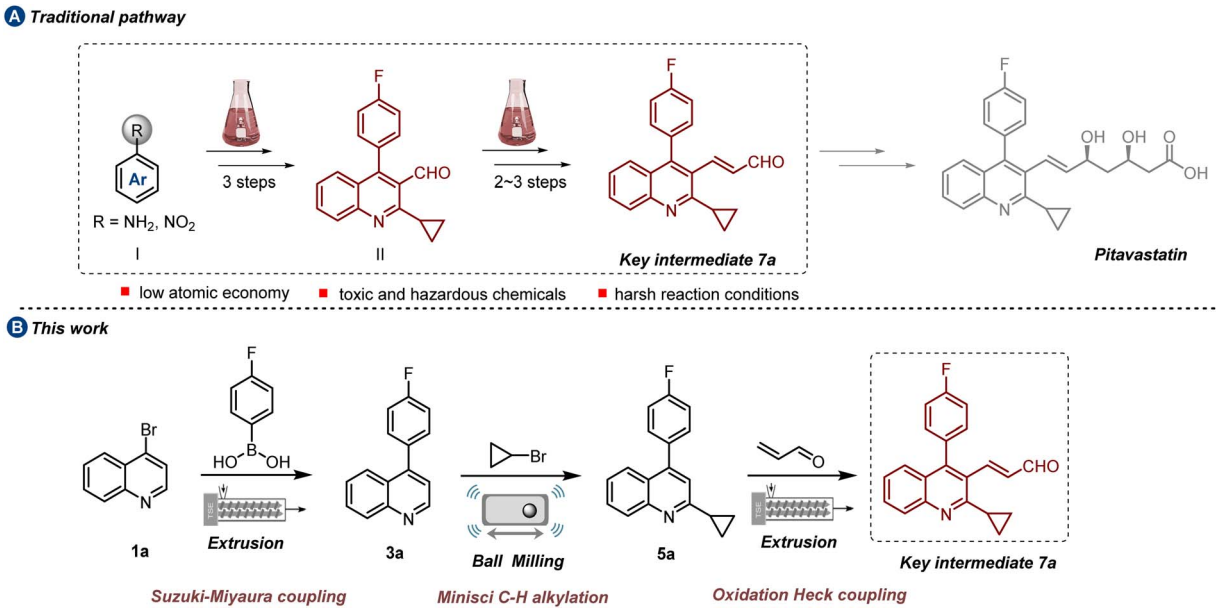

Scheme 1 Background and reaction design of this work.

(anticancer drug) and Pyrimethamine[8j] (anti osteoporosis drug), illustrating the breadth and potential of this greener methodology. Although most mechanochemical researches have been achieved by grinding in ball mills,[9] the shift from small-scale reactions to continuous and scalable mechano-synthesis has attracted great attention of chemists very recently.[10] In 2019, alongside flow chemistry, mechanochemical reactive extrusion, promising in sustainability and scalability, was recognized as one of the top 10 chemical innovations by IUPAC.[11]

As a prevalent form of reactive extrusion, twin-screw extruder (TSE) technology has been widely applied in the preparation of co-crystals, metal organic frameworks (MOFs) and supramolecular porous cages.[12] However, in drug synthesis, there have been only a few sporadic studies.[13] Building upon our previous works on total mechanosynthesis of pharmaceuticals and drug-like compounds,[14] herein we turned our attention to the underexplored scalable mechanochemistry for the green synthesis of PTV.

Results and discussion

The synthetic route depicted in Scheme 1b was chosen for the initial evaluation. Following our proposed pathway, 4-bromoquinoline undergoes a mechanochemical Suzuki–Miyaura coupling reaction with 4-fluorophenylboric acid **2**, resulting in the generation of **3a**. This intermediate subsequently undergoes a one-pot Minisci C–H alkylation reaction with bromocyclopropane **4**, leading to the formation of **5a**.

Ultimately, the pivotal intermediate **7a** is obtained *via* a mechanochemical oxidative Heck reaction. Scalability experiments are carried out at each stage of the process to assess its industrial feasibility. Additionally, due to the essential role of the cyclopropane structure in pharmaceutical compounds, an extensive examination was conducted on the substrate scope of the Minisci reaction, specifically focusing on the direct alkylation of drug-relevant molecules and natural products.

Synthesis of 3a

The synthesis began with the coupling of commercially available 4-bromoquinoline **1a** and fluorophenylboronic acid by classical palladium catalysis, using K_3PO_4 (3.0 equiv.) as a base and NaCl (0.5 mass equiv.) as the grinding auxiliary in a mixer mill (30 Hz, 30 min). Inspired by the works of Kubota and Ito,[15] as well as Browne,[16] which indicated that increasing overall collision energy by inputting of supplementary thermal energy can improve the efficiency of coupling reactions, a heat gun was employed to facilitate the reaction, giving the desired product **3a** in 75–81% isolated yields (Table 1, entries 1 and 2). Due to the cost-effectiveness and lower toxicity of nickel catalysts compared to palladium catalysts,[17] our focus then shifted to nickel-catalysed coupling reactions. Among the tested nickel catalysts, $NiCl_2$(dppp) (10 mol%) provided the best yield of 83% (Table 1, entry 3 *vs.* entries 6 and 7); however, reducing the catalyst loading hindered the reaction. Notably, a decreased amount of **2** contributed positively to the transformation with the best yield of 93% obtained by prolonging the milling time to 60 min (Table 1, entry 4). Modifying either the type (Table 1, entries 8 and 9) or the quantity of the base (K_3PO_4) resulted in unfavourable outcomes (Table 1, entry 5 and Table S1†).

Iron, as one of the most abundant metallic elements on earth, has the advantages of being nontoxic, cost-effective, and environmentally and biologically compatible, making it an ideal green catalyst. In the screening process for catalyst utilizing iron salts, it was observed that ligand-free iron catalysts outperformed the coordinated ones (Table 1, entries 10–13). However, a reduction in the amount of **2** led to a decline in the product yield (Table 1, entry 13, and Table S1†), which was contrasted to nickel catalysis. Considering the benefits of liquid assisted grinding

Table 1 Optimization of Suzuki–Miyaura reaction conditions[a]

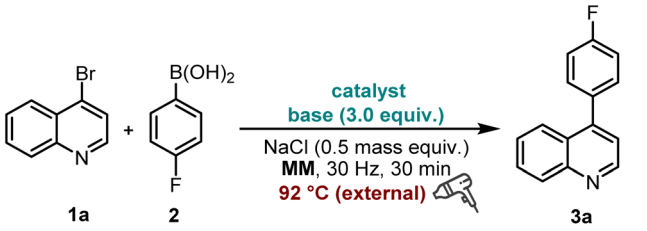

Entry	Catalyst (mol%)	Base (equiv.)	3a [b] (%)
1	$Pd(OAc)_2$ (10)	K_3PO_4 (3)	81
2	$PdCl_2(PPh_3)_2$ (10)	K_3PO_4 (3)	75
3	$NiCl_2$(dppp) (10/8/6)	K_3PO_4 (3)	83/71/56
4	**$NiCl_2$(dppp) (10)**	**K_3PO_4 (3)**	86[c]/80[d]/**93**[c,f]
5	$NiCl_2$(dppp) (10)	K_3PO_4 (2/4)	76/65
6	$NiCl_2(PPh_3)_2$ (10)	K_3PO_4 (3)	75
7	$NiCl_2(PCy_3)_2$ (10)	K_3PO_4 (3)	82
8	$NiCl_2$(dppp) (10)	$K_2CO_3/Na_2CO_3/Cs_2CO_3$ (3)	43/56/39
9	$NiCl_2$(dppp) (10)	$NaHCO_3$/KF/CsF (3)	65/43/70
10	$FeCl_3(PPh_3)_3$ (10)	K_3PO_4 (3)	29
11	$FeCl_3$(dppe)$_3$ (10)	K_3PO_4 (3)	32
12	$FeCl_2$ (10)	K_3PO_4 (3)	33
13	$FeCl_3$ (10)	K_3PO_4/K_2CO_3 (3)	50/53(48[c])
14[e]	**$FeCl_3$ (10/8/6)**	**K_2CO_3 (3)**	**80**/65/48

[a] Reaction conditions unless specified otherwise: **1a** (0.4 mmol), **2** (0.6 mmol), catalyst, base and NaCl (0.5 mass equiv.) were placed in a 15 mL stainless-steel vessel with a stainless-steel ball (d_{MB} = 10 mm), heated by heat-gun, milling in a mixer mill (RETSCH MM 400) for 30 min at 30 Hz. MM = mixer mill. [b] Isolated yields. [c] **2** (0.56 mmol). [d] **2** (0.64 mmol). [e] LAGs (H_2O: 0.08 μL mg^{-1}). [f] Milling for 60 min.

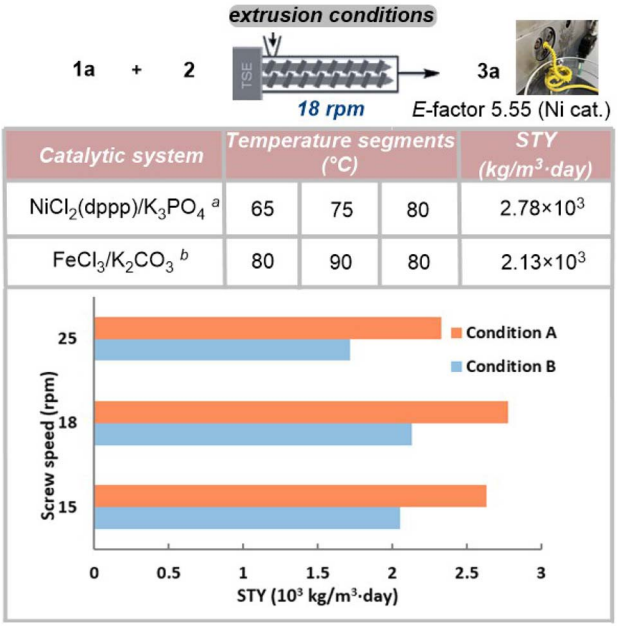

Fig. 1 Extrusion optimization for Suzuki–Miyaura coupling.[a a] Condition A: **1a** (36 mmol), **2** (50.4 mmol), $NiCl_2$(dppp) (10 mol%) and K_3PO_4 (3.0 equiv.) were reacted in a twin-screw extruder (SJZS-7A). Screw speed = 18 rpm, feed rate: 2.63 g min^{-1}, temperature as specified. STY = total product mass (kg)/(reactant volume (m^3) × time (day). [b] Condition B: **1a** (36 mmol), **2** (50.4 mmol), $FeCl_3$ (10 mol%), K_2CO_3 (3.0 equiv.), LAGs (H_2O: 0.08 μL mg^{-1}) and NaCl (10.00 g) were reacted in a twin-screw extruder (SJZS-7A). Screw speed = 18 rpm, feed rate: 2.63 g min^{-1}, temperature as specified. STY = total product mass (kg)/reactant volume (m^3) × time (day).

technology (LAG) in mechanochemistry,[18] where a small amount of liquid can manipulate reactivity, we also applied the LAG protocol in this study (see details in ESI†). The results showcased that the addition of H_2O as a liquid additive (LAGs) along with K_2CO_3 as an alternative base led to a superior yield of up to 80% (Table 1, entry 14). While the yield of iron catalysts may not match that of nickel catalysts, its cost-effectiveness provides an advantage for industrial production. Consequently, further large-scale extrusion studies will investigate the potential industrial applications of both iron and nickel catalyst systems.

Next, we explored the extrusion conditions using a twin-screw extruder (SJZS-7A). A mixture of **1a** (36 mmol, 7.50 g), **2** (50.4 mmol, 7.56 g), iron or nickel catalyst (10 mol%), K_2CO_3 or K_3PO_4 (3.0 equiv.), with or without NaCl and with or without H_2O (0.08 μL mg^{-1}) was manually introduced into the extruder through the feeding port (with a feed rate of 2.63 g min^{-1}). The extrusion process was performed at a screw rotation rate of 18 rpm and with three-stage heating temperatures (Fig. 1). Following an optimization study of this three-stage heating protocol, it was determined that the nickel catalytic reaction exhibited the best transformation at temperatures of 65 °C, 75 °C, 80 °C, while the iron catalytic reaction required higher temperatures (80 °C, 90 °C, 80 °C) to achieve optimal results. Subsequent experiments revealed that lower screw speeds of 18 and 15 rpm were more effective compared to 25 rpm. This improvement in efficiency at lower speeds can be attributed to the longer residence time [Ni cat. (from 11 min to 15 min); Fe cat. (from 13 min to 15 min)] of the reactants within the extruder, which facilitates enhanced conversion of the reactants. Ultimately, the highest Space-Time Yield (STY) values were determined for the Ni catalyst and Fe catalyst, respectively. The Ni catalyst achieved an STY of 2.78 × 10^3 kg per m^3 per day (*E*-factor 5.55, see details in ESI†), while the Fe catalyst demonstrated an STY of 2.13 × 10^3 kg per m^3 per day. It should be noted that approximately 18 g of extrudate (out of the total 40 g blend loaded) was processed before the system reached a steady state. Losses in continuous processes are a frequent occurrence, with their significance diminishing notably as material inputs scale up.[19]

Synthesis of 5a

Our recent study demonstrated the generation of alkyl radicals through the mechanochemical interaction of alkyl halides with freshly prepared magnesium surfaces, enabling the Minisci-type alkylation of pyrimidine[14c] and pyridine[8] derivatives. Consequently, we envisage employing this methodology for the synthesis of PTV, through the C–H alkylation reaction of *p*-fluorophenylquinoline **3a** with bromocyclopropane **4**. The investigation commenced by employing these two substrates, resulting in an 18% yield of **5a** with the presence of 2 equiv. of magnesium along with Na_2SO_4 (1.0 g) as the grinding auxiliary

(Table 2, entry 2). Control experiments confirmed the necessity of magnesium for the reaction (Table 2, entry 1), demonstrating the significant impact of its quantity on the product yield (Table 2, entry 2). Other grinding auxiliary gave inferior results (Table 2, entry 3) and the experiments indicated the generation of a certain amount of defluorinated by-product alongside the desired product. In an effort to reduce these by-products, potassium fluoride (KF) was introduced as a grinding auxiliary. However, contrary to expectations, KF not only failed to inhibit the formation of by-products but also decreased the yield of the desired product notably (Table 2, entries 3 and 4). Interestingly, optimizing the amount of grinding auxiliary Na_2SO_4 (0.9 g) led to a substantial increase in the product yield up to 64%, especially when the amount of bromocyclopropane **4** is reduced from 5 to 4 equivalents (Table 2, entries 5 and 6; Tables S5 and S6†), however further decrease its amount did not give any help for this transformation (Table S5,† entry 9). To further demonstrate the efficiency and synthetic utility of this methodology (Scheme 2), a large-scale experiment (8 mmol) was conducted involving the reaction of **3a** and **4** in a 50 mL stainless-steel ball-milling jar equipped with two stainless-steel balls (d_{MB} = 14 mm). This procedure successfully produced the desired compound **5a** with a satisfactory yield (51%, *E*-factor 2.92/15.65, see details in ESI†). The cyclopropyl motif plays a crucial role in bioactive molecules and natural products.[20] Research indicates that incorporating a cyclopropane fragment enhances drug properties such as lipid solubility, specificity, and resistance to metabolic degradation.[21] Given the importance of the cyclopropyl motif in medicinal chemistry, this study further investigates the substrate scope and adaptability of heteroarenes as potential drug structural components under the optimal conditions (Fig. 2). A range of 4-arylquinolines with both electron-donating and electron-withdrawing substituents at different positions on the phenyl ring successfully underwent

Table 2 Optimization of Minisci C–H alkylation reaction conditions[a]

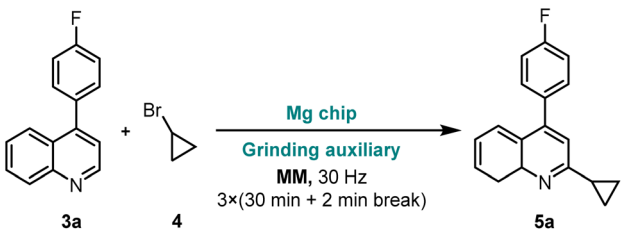

Entry	Mg chip (equiv.)	Grinding auxiliary (g)	**5a** [b] (%)
1	—	Na_2SO_4 (1.0)	n.d.
2	2.0/3.0/4.0	Na_2SO_4 (1.0)	18/43/37
3	3.0	NaCl/silica gel/KF (1.0)	n.d./n.d./15
4	3.0	KF : Na_2SO_4 = 3 : 7/2 : 8 (1.0)	28/32
5	3.0	Na_2SO_4 (0.8/0.9)	45/53
6[c]	**3.0**	**Na_2SO_4 (0.9)**	**64**

[a] Reaction conditions: **3a** (0.2 mmol), **4** (1.0 mmol), Mg chip (3.0 equiv.) and Na_2SO_4 (1.0 g) were placed in a 15 mL stainless-steel vessel with a stainless-steel ball (d_{MB} = 12 mm), milling in a mixer mill (RETSCH MM 400) for [3 × (30 min + 2 min break)] at 30 Hz. MM = mixer mill. [b] Isolated yields. [c] **4** (0.8 mmol), a stainless-steel ball (d_{MB} = 14 mm).

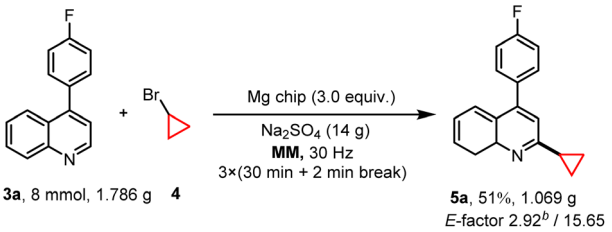

Scheme 2 Gram-scale for the Minisci C–H alkylation reaction.[a] [a] Reaction conditions: **3a** (8 mmol), **4** (16 mmol), Mg chip (3.0 equiv.) and Na_2SO_4 (14 g) were placed in a 50 mL stainless-steel vessel with two stainless-steel balls (d_{MB} = 14 mm), milling in a mixer mill (RETSCH MM 400) for [3 × (30 min + 2 min break)] at 30 Hz. MM = mixer mill. [b] Without grinding auxiliary.

reactions with bromocyclopropane **4**, giving the desired products **5a–5f** in 48–51% yields. 4-Methylquinoline (**3g**) and 4-bromoquinoline (**3h**) also served as compatible substrates, albeit resulting in relatively lower yields. Encouragingly, the reaction scope extended to other valuable heteroarenes such as 4-methoxypyridine (**4i**), 4-*tert*-butylpyridine (**4j**), 4-methylpyrimidine (**4k**), benzothiazole (**4l**), and the challenging *N*-methyl-1*H*-indazole (**4m**).[22] Notably, the potential of this method in the late-stage modification of drug-relevant molecules and natural products was demonstrated by utilizing caffeine, theophylline and a clioquinol derivative as substrates, resulting in products **5n–5p** with synthetically acceptable yields.

Synthesis of the key intermediate 7a

The final step involves the conversion of **5a** to 3-(2-cyclopropyl-4-(4-fluorophenyl)quinolin-3-yl)acrylaldehyde **7a**, which is the key intermediate in the synthesis of PTV (Table 3, see details in Tables S9–S11†). Initially, this transformation was carried out using $Pd(OAc)_2$ (10 mol%) as the catalyst, 1,10-phenanthroline (13 mol%) as the ligand, Ag_2CO_3 (1.0 equiv.) as the oxidant, DMF (0.12 μL mg^{-1}) as LAGs, and Na_2SO_4 (0.5 g) as the grinding auxiliary in a mixer mill (RETSCH MM 400) equipped with a heat gun operating at 30 Hz for (2 × 30) min, offering the desired product in 39% yield (Table 3, entry 1). The investigation of alternative palladium catalysts (Pd$[O_2C(CH_3)_3]_2$, $Pd(acac)_2$, and $PdCl_2(PPh_3)_2$) or silver oxidants (Ag_2CO_3, Ag_2O, CF_3SO_2OAg, $AgBF_4$, AgOAc, Ag_2CO_3 : $Cu(OAc)_2$ = 1 : 1, and Ag_2CO_3 : $CuCO_3$ = 1 : 1) revealed a significant reduction in yield (Table 3, entries 2–4). Moreover, altering the catalyst loading (from 10% to 8 mol%) and stoichiometric amount of oxidant (from 1.0 equiv. to 1.5 equiv.) gave comparative results (Table 3, entry 5). Further experiments demonstrated that 1,10-phenanthroline as the ligand exhibited superior performance compared to other ligands (Table 3, entry 6). Switching the grinding auxiliary from Na_2SO_4 to silica gel/$NaHCO_3$/Na_2CO_3, or changing the LAGs from DMF to MeCN/EtOAc/DMSO/hexane all led to diminished yields (Table 3, entries 7 and 8). The optimal quantities for these two additives were found to be 0.5 g and 0.12 μL mg^{-1}, respectively (Table 3, entry 9 and Table S10†). Lastly, adjusting the substrate ratios to 1 : 1/1 : 2 did not improve the formation of the coupling product (Table 3, entry 10).

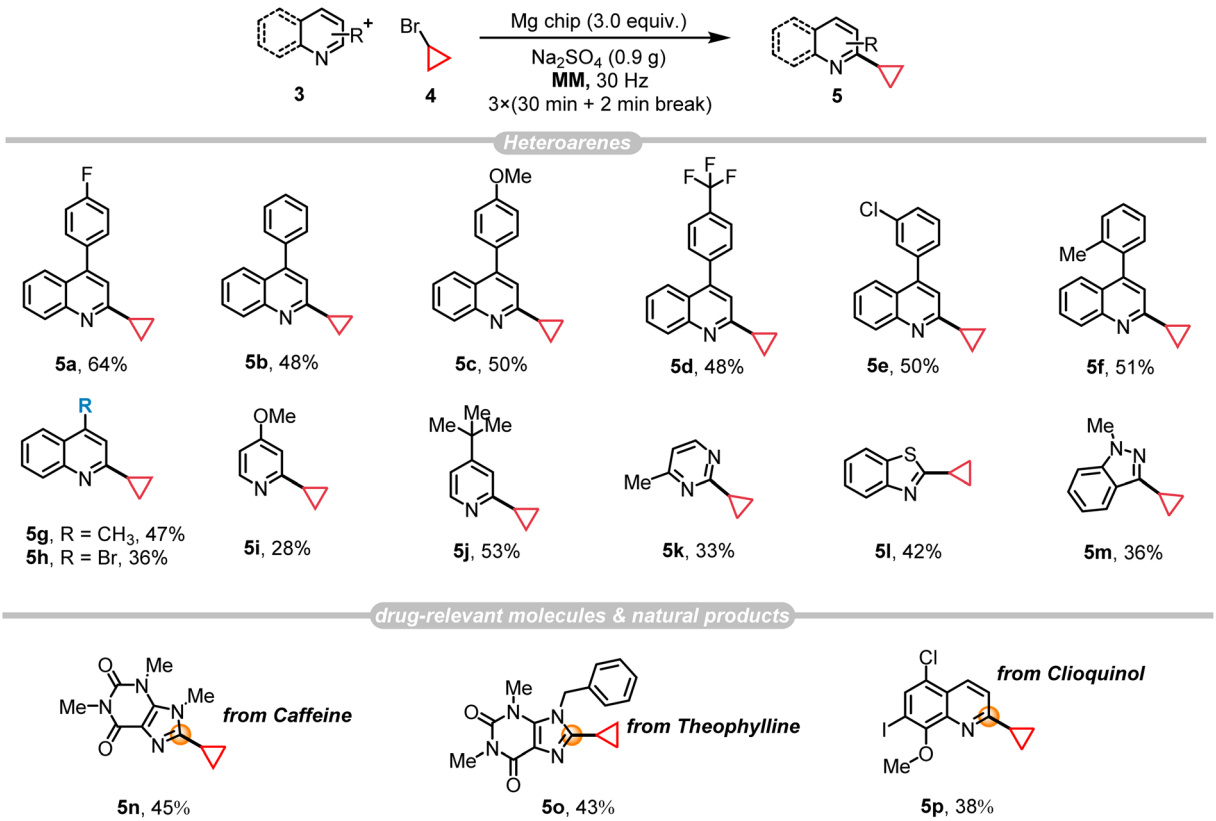

Fig. 2 Substrate scope for Minisci C–H alkylation reaction.[a a] Reaction conditions: **3** (0.2 mmol), **4** (0.8 mmol), Mg chip (3.0 equiv.) and Na_2SO_4 (0.9 g) were placed in a 15 mL stainless-steel vessel with a stainless-steel ball (d_{MB} = 14 mm), milling in a mixer mill (RETSCH MM 400) for [3 × (30 min + 2 min break)] at 30 Hz. MM = mixer mill. Isolated yield.

After establishing the optimal conditions through mixer milling tests, our study advanced to investigate the extrusion parameters suitable for large-scale reactions using a twin-screw extruder (SJZS-7A) (Fig. 3). Scaling our methodology up by 80-fold to a 32 mmol scale of quinoline starting material **5a** involved manual mixing of all the reactants (**5a,** 16 mmol **6,** and

Table 3 Optimization of oxidative Heck reaction conditions[a]

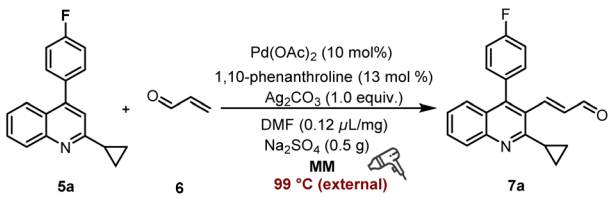

Entry	Deviation from standard conditions	Yield[b] (%)
1	None	43
2	$Pd[O_2C(CH_3)_3]_2$/$Pd(acac)_2$/$PdCl_2(PPh_3)_2$ instead of $Pd(OAc)_2$	24/27/30
3	Ag_2CO_3/Ag_2O/CF_3SO_2OAg/$AgBF_4$/AgOAc instead of Ag_2CO_3	23/12/18/n.d./n.d.
4	Ag_2CO_3 : $Cu(OAc)_2$ (1 : 1)/Ag_2CO_3 : $CuCO_3$ (1 : 1) instead of Ag_2CO_3	27/trace
5	8 mol% instead of 10 mol% of $Pd(OAc)_2$/1.5 eq. instead of 1.0 eq. of Ag_2CO_3	35/34
6	CEMTPP/DPPE instead of 1,10-phenanthroline	32/31
7	Silica gel/$NaHCO_3$/Na_2CO_3 instead of Na_2SO_4	32/n.d./trace
8	MeCN/EtOAc/DMSO/hexane instead of DMF	23/18/25/22
9	0.10/0.08 μL mg^{-1} of DMF	34/28
10	1.0 eq./2.0 eq. of **6**	28/34

[a] Reaction conditions: **5a** (0.4 mmol), **6** (0.6 mmol), $Pd(OAc)_2$ (10 mol%), 1,10-phenanthroline (13 mol%), Ag_2CO_3 (1.0 equiv.) DMF (0.12 μL mg^{-1}) and Na_2SO_4 (0.5 g) were placed in a stainless-steel vessel (15 mL) with a stainless-steel ball (d_{MB} = 10 mm), milling in a mixer mill (RETSCH MM 400) at 30 Hz for (2 × 30) min. [b] Isolated yields. MM = mixer mill. n. d. = not detected. CEMTPP = ethoxycarbonylmethylene triphenylphosphorane. DPPE = 1,2-bis(diphenylphosphine)ethane.

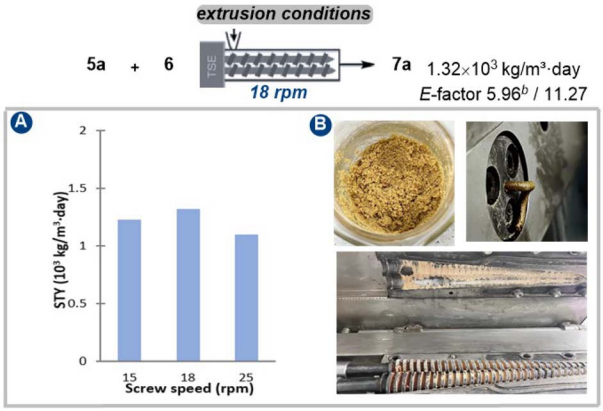

Fig. 3 Extrusion optimization for oxidative Heck reaction conditions.[a] [a] Reaction conditions: **5a** (32 mmol), **6a** (16 mmol), $Pd(OAc)_2$ (10 mol%), 1,10-phenanthroline (13 mol%), Ag_2CO_3 (1.0 equiv.), DME (0.12 μL mg^{-1}) and Na_2SO_4 (20 g) were reacted in a twin-screw extruder (SJZS-7A). Screw speed = 18 rpm, feed rate: 2.63 g min^{-1}, temperature as specified. STY = total product mass (kg)/reactant volume (m^3) × time (day).

32 mmol Ag_3CO_3), catalyst (3.2 mmol $Pd(OAc)_2$/4.2 mmol 1,10-phenanthroline), and additives (20 g Na_2SO_4 and 0.12 μL mg^{-1} DMF) with a spatula, then feeding them into the extruder through a hopper over 15 minutes. The initial investigation was started by adjusting the three-stage heating temperatures to establish steady-state conditions ensuring the mass neither too wet nor too dry. In this context, our research revealed that the optimal temperature was determined to be 90 °C, 105 °C, and 80 °C, respectively (Table S12†). Subsequent analysis focused on the impact of reducing the screw speed from 25 to 18 rpm for mixtures processed at 90°C–105°C–80 °C, consequently increasing the residence time (from 15 min to 18 min) in the extruder barrel. Thereby, an optimal Space-Time Yield (STY) of 1.32×10^3 kg per m^{-3} per day was achieved (*E*-factor 5.96/11.27, see details in ESI†).

A comprehensive comparison was then carried out between the total mechanosynthesis methodology and the conventional route for the preparation of the pivotal intermediate **7a** of pitavastatin (Table 4, see details in Fig. S1–S4†). The findings unmistakably established that the total mechano-synthesis strategy introduced herein outperformed the traditional process in both time efficiency and procedural economy, necessitating the fewest steps. Furthermore, the environmental factor (*E*-factor) was meticulously computed for every individual step within the ESI.† These computations revealed that three stages within the total mechano-synthesis displayed relatively low *E*-factor values, ranging from 2.92 to 15.65.

Table 4 Comparison of the synthetic routes of **7a**

Method	Steps	Time (h)	Total yield (%)
Mechanochemical method	3	10.8	25.6[a]
Traditional method 1	7	51.0	17.0
Traditional method 2	6	68.5	17.7
Traditional method 3	6	202.0	15.5

[a] The yield derived from small-scale experimental studies, wherein the Suzuki–Miyaura cross-coupling reaction is catalyzed by utilizing nickel metal.

Conclusion

In summary, we have successfully developed a novel, environmentally friendly, and industrially promising mechanochemical route for the green synthesis of the key intermediate **7a** of pitavastatin (PTV), overcoming environmental issues associated with conventional methods. Following meticulous optimization, the synthesis was accomplished in a streamlined three-step processes (Suzuki–Miyaura coupling, Minisci C–H alkylation, and oxidation Heck coupling). Significantly, two of these steps were effectively upscaled utilizing continuous-flow extrusion technology, with the second step demonstrating its scalability at the gram-scale level. Moreover, given the substantial therapeutic significance of cyclopropyl moieties, we probed the versatility of the mechanochemical Minisci methodology, revealing its promising potential for the targeted cyclopropylation of active pharmaceutical compounds. The developed process underscores the untapped potential of mechanochemistry in drug synthesis, particularly when integrated into continuous flow systems that offer shortened production times, fewer procedural steps, solvent-free operations, and enhanced product yields. Consequently, this advancement contributes to a more environmentally sustainable and resource-efficient synthesis paradigm, aligning with contemporary imperatives for greener pharmaceutical synthesis.

Author contributions

JB suggested the idea, YH and ZH performed the experiments and processed the data. WK and JB supervised the project. Writing – review, and editing were conducted by YH and JB. All authors have read and approved the final manuscript.

Conflicts of interest

There are no conflicts to declare.

Acknowledgements

We gratefully acknowledge the Zhejiang Provincial Natural Science Foundation of China (No. LY23B060005), the National Natural Science Foundation of China (No. 21978270), and National Key R&D Program of China 2021YFC2101000 for financial support.

References

1 A. Sahebkar, N. Kiaie, A. M. Gorabi, M. R. Mannarino, V. Bianconi, T. Jamialahmadi, M. Pirro and M. Banach, *Prog. Lipid Res.*, 2021, **84**, 101127.
2 A. Ramadan and A. Elnour, *J. Pharm. BioAllied Sci.*, 2022, **14**, 72–80.

3 K. Tajiri, N. Shimojo, S. Sakai, T. Machino-Ohtsuka, K. Imanaka-Yoshida, M. Hiroe, Y. Tsujimura, T. Kimura, A. Sato, Y. Yasutomi and K. Aonuma, Cardiovasc, *Drugs Ther.*, 2013, **27**(5), 413–424.

4 (*a*) Y. N. Fuiikawa and M. N. Suzuki, EP Pat., 0304063, 1989; (*b*) Z. Časar, *Curr. Org. Chem.*, 2010, **14**, 816–845; (*c*) J. Wang, M. Sanchez-Rosello, J. L. Acena, C. del Pozo, A. E. Sorochinsky, S. Fustero, V. A. Soloshonok and H. Liu, *Chem. Rev.*, 2014, **114**, 2432–2506.

5 (*a*) Y. Ohara and M. Suzuki, World Pat., 2000005213A1, 2000; (*b*) Y. Ohara, M. Suzuki and Y. Yanagawa, EP Pat., 0520406A1, 1992.

6 (*a*) Y. Wan and X. Hu, *Org. Lett.*, 2022, **24**, 5797–5801; (*b*) C. Counceller, C. Eichman, B. Wray and J. Stambuli, *Org. Lett.*, 2008, **10**, 1021–1023; (*c*) P. Li, L. Yu, X. Zhang and M. Shi, *Org. Lett.*, 2018, **20**, 4516–4520; (*d*) Z. Chasar, D. Cituock and M. Jukic, CN Pat., 103119022B, 2016; (*e*) C. M. Counceller, C. C. Eichman, B. C. Wray and J. P. Stambuli, *Org. Lett.*, 2008, **10**, 1021–1023; (*f*) Z. Li and S. Li, CN Pat., 104496898A, 2015.

7 For selected reviews: (*a*) G.-W. Wang, *Chem. Sci. Rev.*, 2013, **42**, 7668–7700; (*b*) S.-E. Zhu, F. Li and G.-W. Wang, *Chem. Sci. Rev.*, 2013, **42**, 7535–7570; (*c*) J. G. Hernández and C. Bolm, *J. Org. Chem.*, 2017, **82**, 4007–4019; (*d*) J.-L. Do and T. Friščić, *ACS Cent. Sci.*, 2017, **3**, 13–19; (*e*) T. Friščić, C. Mottillo and H. M. Titi, *Angew. Chem., Int. Ed.*, 2020, **59**, 1018–1029; (*f*) F. Cuccu, L. De Luca, F. Delogu, E. Colacino, N. Solin, R. Mocci and A. Porcheddu, *ChemSusChem*, 2022, **15**, e202200362; (*g*) V. Martinez, T. Stolar, B. Karadeniz, I. Brekalo and K. Užarević, *Nat. Rev. Chem.*, 2023, **7**, 51–65; (*h*) J. Reynes, V. Isoni and F. García, *Angew. Chem., Int. Ed.*, 2023, **62**, e202300819; (*i*) C. G. Avila-Ortiz and E. Juaristi, *Molecules*, 2020, **25**, 3579; (*j*) E. Juaristi and C. G. Ávila Ortiz, *Synthesis*, 2023, **55**, 2439–2459.

8 For selected reviews: (*a*) X. Yang, C. Wu, W. Su and J. Yu, *Eur. J. Org Chem.*, 2022, e202101440; (*b*) F. Cuccu, L. De Luca, F. Delogu, E. Colacino, N. Solin, R. Mocci and A. Porcheddu, *ChemSusChem*, 2022, **15**, e202200362; (*c*) O. Bento, F. Luttringer, T. Mohy El Dine, N. Pétry, X. Bantreil and F. Lamaty, *Eur. J. Org Chem.*, 2022, e202101516; for selected examples; (*d*) M. Pérez-Venegas and E. Juaristi, *ACS Sustainable Chem. Eng.*, 2020, **8**, 8881–8893; (*e*) L. Konnert, B. Reneaud, R. M. de Figueiredo, J.-M. Campagne, F. Lamaty, J. Martinez and E. Colacino, *J. Org. Chem.*, 2014, **79**, 10132–10142; (*f*) L. Konnert, M. Dimassi, L. Gonnet, F. Lamaty, J. Martinez and E. Colacino, *RSC Adv.*, 2016, **6**, 36978–36986; (*g*) A. Porcheddu, F. Delogu, L. De Luca and E. Colacino, *ACS Sustain. Chem. Eng.*, 2019, **7**, 12044–12051; (*h*) D. Tan, V. Štrukil, C. Mottillo and T. Friščić, *Chem. Commun.*, 2014, **50**, 5248–5250; (*i*) T. Portada, D. Margetić and V. Štrukil, *Molecules*, 2018, **23**, 3163; (*j*) J. Yu, Z. Hong, X. Yang, Y. Jiang, Z. Jiang and W. Su, *Beilstein J. Org. Chem.*, 2018, **14**, 786–795; (*k*) C. Wu, T. Ying, H. Fan, C. Hu, W. Su and J. Yu, *Org. Lett.*, 2023, **25**, 2531–2536.

9 For selected examples: (*a*) A. Stolle, R. Schmidt and K. Jacob, *Faraday Discuss.*, 2014, **170**, 267C286; (*b*) J. L. Do, C. Mottillo, D. Tan, V. Strukil and T. Friscic, *J. Am. Chem. Soc.*, 2015, **137**, 2476–2479; (*c*) V. S. Pfennig, R. C. Villella, J. Nikodemus and C. Bolm, *Angew. Chem., Int. Ed.*, 2022, **61**, e202116514; (*d*) L. Li, C. Niu and G.-W. Wang, *Chin. J. Chem.*, 2022, **40**, 2539–2545; (*e*) G. Shao, C. Niu, H.-W. Liu, H. Yang, J.-S. Chen, Y.-R. Yao, S. Yang and G.-W. Wang, *Org. Lett.*, 2023, **25**, 1229–1234; (*f*) R. Takahashi, P. Gao, K. Kubota and H. Ito, *Chem. Sci.*, 2023, **14**, 499–505.

10 (*a*) Q. Cao, J. L. Howard, D. E. Crawford, S. L. James and D. L. Browne, *Green Chem.*, 2018, **20**, 4443–4447; (*b*) K. J. Ardila-Fierro and J. G. Hernández, *ChemSusChem*, 2021, **14**, 2145–2162; (*c*) R. R. A. Bolt, J. A. Leitch, A. C. Jones, W. I. Nicholson and D. L. Browne, *Chem. Soc. Rev.*, 2022, **51**, 4243–4260; (*d*) R. R. A. Bolt, S. E. Raby-Buck, K. Ingram, J. A. Leitch and D. L. Browne, *Angew. Chem., Int. Ed.*, 2022, **61**, e202210508; (*e*) Q. Cao, D. E. Crawford, C. Shi and S. L. James, *Angew. Chem., Int. Ed.*, 2020, **59**, 4478–4483.

11 F. Gomollón-Bel, *Angew. Chem., Int. Ed.*, 2019, **41**, 12–17.

12 (*a*) D. E. Crawford, *Beilstein J. Org. Chem.*, 2017, **13**, 65–75; (*b*) D. E. Crawford and J. Casaban, *Adv. Mater.*, 2016, **28**, 5747–5754; (*c*) D. Crawford, J. Casaban, R. Haydon, N. Giri, T. McNally and S. L. James, *Chem. Sci.*, 2015, **6**, 1645–1649.

13 (*a*) E. Colacino, A. Porcheddu, C. Charnay and F. Delogu, *React. Chem. Eng.*, 2019, **4**, 1179–1188; (*b*) D. E. Crawford, A. Porcheddu, A. S. McCalmont, F. Delogu, S. L. James and E. Colacino, *ACS Sustainable Chem. Eng.*, 2020, **8**, 12230–12238; (*c*) I. Sović, S. Lukin, E. Meštrović, I. Halasz, A. Porcheddu, F. Delogu, P. C. Ricci, F. Caron, T. Perilli, A. Dogan and E. Colacino, *ACS Omega*, 2020, **5**, 28663–28672.

14 (*a*) J. Yu, P. Ying, H. Wang, K. Xiang and W. Su, *Adv. Synth. Catal.*, 2020, **362**, 893–902; (*b*) J. Yu, X. Yang, C. Wu and W. Su, *J. Org. Chem.*, 2020, **85**, 1009–1102; (*c*) C. Wu, T. Ying, X. Yang, W. Su, A. V. Dushkin and J. Yu, *Org. Lett.*, 2021, **23**, 6423–6428; (*d*) H. Shou, Z. He, G. Peng, W. Su and J. Yu, *Org. Biomol. Chem.*, 2021, **19**, 4507–4514; (*e*) X. Yang, H. Wang, Y. Zhang, W. Su and J. Yu, *Green Chem.*, 2022, **24**, 4557–4565; (*f*) K. Xiang, P. Ying, T. Ying, W. Su and J. Yu, *Green Chem.*, 2023, **25**, 2853–2862; (*g*) J. Yu, H. Chen, Z. Zhang, Y. Fang, T. Ying and W. Su, *Green Chem.*, 2024, **26**, 6570–6577.

15 (*a*) Y. Gao, C. Feng, T. Seo, K. Kubota and H. Ito, *Chem. Sci.*, 2022, **13**, 430–438; (*b*) R. Takahashi, A. Hu, P. Gao, Y. Gao, Y. Pang, T. Seo, S. Maeda, J. Jiang, H. Takaya, K. Kubota and H. Ito, *Nat. Commun.*, 2021, **12**, 6691; (*c*) R. Takahashi, A. Hu, P. Gao, Y. Gao, Y. Pang, T. Seo, S. Maeda, J. Jiang, H. Takaya, K. Kubota and H. Ito, *Angew. Chem., Int. Ed.*, 2022, **61**, e202210508.

16 (*a*) R. R. A. Bolt, S. E. Raby-Buck, K. Ingram, J. A. Leitch and D. L. Browne, *Angew. Chem., Int. Ed.*, 2022, **61**, e202210508; (*b*) R. R. A. Bolt, S. E. Raby-Buck, K. Ingram, J. A. Leitch and D. L. Browne, *Angew. Chem.*, 2022, **134**, e202210508.

17 B. M. Rosen, K. W. Quasdorf, D. A. Wilson, N. Zhang, A.-M. Resmerita, N. K. Garg and V. Percec, *Chem. Rev.*, 2011, **111**, 1346–1416.

18 P. Ying, J. Yu and W. Su, *Adv. Synth. Catal.*, 2021, **363**, 1246–1271.

19 R. H. Hastings, M. M. Mokhtar, A. Ruggles, C. Schmidt, D. Bourdeau, M. C. Haibach, H. Geneste, J. Mack, S. S. Co and I. R. Speight, *Org. Process Res. Dev.*, 2023, **27**, 1667–1676.
20 (*a*) L.-Q. Sun, F. McPhee and P. M. Scola, *J. Med. Chem.*, 2016, **59**, 8042–8060; (*b*) N. A. Meanwell, *J. Med. Chem.*, 2016, **59**, 7311–7351.
21 (*a*) L. A. Dawson, *Bioorg. Med. Chem. Lett.*, 2009, **19**, 837–840; (*b*) Y. Yoshida, Y. Naoe, T. Terauchi, F. Ozaki, T. Doko, A. Takemura, T. Tanaka, K. Sorimachi, C. T. Beuckmann, M. Suzuki, T. Ueno, S. Ozaki and M. Yonaga, *J. Med. Chem.*, 2015, **58**, 4648–4664.
22 S. Faarasse, S. El Kazzouli, F. Suzenet and G. Guillaumet, *J. Org. Chem.*, 2018, **83**, 12847–12854.